Powder flow behavior governed by the surface properties of glass beads

Shirin Enferad, Salvatore Pillitteri, Geoffroy Lumay, Claire Gaiani, Sebastien Kiesgen de Richter, Michaël Marck, Syrym Umbetov, Nicolas Vandewalle, Mathieu Jenny

Powder flow behavior governed by the surface properties of glass beads

Shirin Enferard[1,2], Salvatore Pillitteri[3], Geoffroy Lumay[3], Claire Gaiani[2], Sebastien Kiesgen De Richter[1], Michaël Marck[3], Syrym Umbetov[1], Nicolas Vandewalle[3], Mathieu Jenny[1]

[1]Université de Lorraine, Laboratoire d'Energétique et de Mécanique Théorique et Appliqué (LEMTA), CNRS, UMR 7563, Vandoeuvre-lés-Nancy, F-54500, France.

[2]Université de Lorraine, Laboratoire d'Ingénierie des Biomolécules (LIBio), 2 avenue de la Forêt de Haye, TSA 40602, 54518 Vandoeuvre-lès-Nancy, France.

[3]GRASP, Institute of Physics B5a, University of Liège, B4000 Liège, Belgium.

[*]Corresponding author.

Abstract

Powder rheology and its sensitivity to surrounding environmental condition by controlling the surface properties of the particles is one of the major challenges of the powder industries. Indeed, handling large quantities needs powders with good flowability, adequate compressibility and few electrostatic charges. We have performed a chemical treatment in order to obtain hydrophobic glass beads and its bulk behavior has been compared with raw glass beads depending on the humidity. We characterized flow properties under different processing equipments. We observed that by performing hydrophobic surface treatment sensitivity of glass beads reduced to the humidity. Furthermore, the influence of the electrostatic charges was an undeniable factor in increasing the viscosity of hydrophobic glass beads and consequently lowering its flowability in front of raw glass beads; at low shear rate. At high shear rate, the powders presented similar behaviors.

Keywords: Flowability, glass bead, hydrophobic formulation, humid control

1. Introduction

Powders are omnipresent in our daily life and they are extensively used in various industries such as pharmaceutical, cosmetics, chemical, food and construction. Despite numerous studies on powder rheology [1, 2, 3, 4, 5, 6, 7] their behavior is not fully understood, due to their complexity. In fact, the flow behavior of a powder depends on many factors including surface properties, size, shape of particles [8] and environmental conditions such as humidity [9].

However, understanding the powder's flowability is one the most important objectives in powder industries. Indeed, it can allow them to anticipate the powder's characteristics by knowing the condition that they encounter during process. In order to identify the pertinent parameters

governing the powder's flow, using different test methods that represent the state of stress and strain rate of interest is very important. These methods can provide different points of view and indices to assess powder flowability with several mechanical and dynamical conditions that have been explained in the following.

It is known that the Hausner ratio is an efficient and rapid method to estimate the powder behavior based on bulk density [10], Hausner ratio correlated to the ratio between settled bulk density and tapped bulk density. It has been reported that low compressible powders have the best flowability [11]. Similarly, a study on copper powder indicated that the Hausner ratio can be representative of friction condition between particles [12].

Apparition of powder electrostatic charges as a result of particle-particle interaction and powders interaction with manipulating equipment during powder process is a know phenomena in industries. In addition, depending on the different surface chemical formulation of powders, the electrostatic charge can increase or decrease which impacts the powder bulk behavior [13, 14]. Whereby, an increase in powder electrostatic charge can lower its flowability [15, 16]. Powder characterization based on their electrostatic charge is of great interest [17, 18, 19].

Moreover, rotating drum is a method to characterize the macroscopic properties of powders under aeration condition, it fluidizes the powder and reports evolution of cohesion under rotation [6]; this technique measures powder flow at high shear rate condition. Furthermore, one of the most used methods in industry is applying vibration during process. This technique optimizes powder flowability consequently enhances saving energy. In addition, this method is convenient to control the different steps of industrial process consisting of feeding, conveying and even parts of the equipment such as hopper, etc [20, 21]. The mentioned technique has been studied recently by implementing a rheometer attached to a shaker [21]. Based on vibrational rheology, the powder flow can be assessed at low shear rate condition.

On the other side, studying and understanding the influence of environmental condition like as humidity on powder behavior is very significant and of great interest. A large number of theoretical and experimental studies in the literature are devoted to figuring out the link between air humidity and powder flow behavior [22, 23, 24, 25, 26, 27, 28, 29, 30]. A decrease in flowability with increasing relative air humidity has been reported for granular material [26, 27, 29] and food powders [25, 30].

This paper focuses on studying the influence of surface treatment on powder flowability

and sensitivity of powder flowability to the external condition. Therefore, first in section III.A, the influence of surface treatment on the behavior of raw and hydrophobic glass beads has been studied in ambient temperature without humid control. Different methods utilised to figuring out the macroscopic flow and the rheology of powders under different processing dynamics. Then in section III.B, the influence of humidity on powder behavior has been studied. In this case, two different methods of humid control and powder rheology utilized to characterize the powders and finally their results have been compared.

First, the humid control was done inside a rotating drum with humid-air controlled flow. The powders were kept for 1 h in each selected humid range.

A second experiment with a different humid control method was conducted at the same time, in order to compare and to link the dependency of the humidity on the shear rate with the electrostatic charge of powders and their cohesion.

In this case, the powders were kept in a humid chamber for 72 h at 20°C in a given humidity ranging from 35 % up to 90 % RH. The humid control time kept long enough to be sure that the powders took enough humidity at each humid value and at the end of humid control the humidity value of powders were confirmed by TH200 thermoconstanter. Then the rheology of powders was performed in a dry room in ambient temperature during maximum 30 min of measurement. The apparent viscosity of powders has been measured with Discovery HR3-Rheometer. The rheometer was attached to a shaker in order to ensure a reproducible packing state and collect data at low shear rate condition. All results have been collected by imposing shear stress.

2. Materials and Methods

In the following, the implemented materials and the different methods for characterizing powders have been explained. The purpose of using different methods is to characterize powders under different processing dynamics and to observe the influence of treatment and mainly the effect of humidity on powders flowability. Therefore, two series of tests have been performed on raw and hydrophobic glass beads. First, the characterization measurements have been done by implementing the Granutools equipments. The packing dynamics of powders has been measured with the GranuPack, the powder electrostatics charge studied with the GranuCharge and the

powder flowability and cohesion measured with GranuDrum equipment. During performing measurements with the Granutools equipments, the humidity and temperature were kept constant at 37-44 % RH and 22°C, respectively. All Granutools measurements have been repeated three times.

Then the study of influence of wide range of humidity has been done on powders with the GranuDrum and the GranuCharge. These results have been confronted with the measurements of the powder behavior (after longer humid control) under vibrational rheology with Discovery HR3-Rheometer which provides possibility of powder flow at low shear rate where the cohesion of powders play a role in their flowability. The goal here was to observe clearly the effect of humidity on powders behaviors based on the strength of their surface cohesion depending on their surface treatment.

2.1. Powders preparation and conditioning

In this study, glass beads of type S 90-150 μm have been used. Hydrophobic surface treatment has been done on the glass beads. With the purpose of preparing hydrophobic surface treatment on the glass beads [31, 32], first the hydrophilic surface treatment has been prepared. The hydrophilic treatment [31] was achieved with a 3:1 mixture of sulfuric acid and hydrogen peroxide. First, 50 g of glass beads was put in a beaker and immersed in sulfuric acid then hydrogen peroxide was gently added. The mixture was kept 4 h at ambient temperature (20°C) under extractor hood. After that, the glass beads was washed with distilled water then silanization protocol has been followed. The silanization of glass beads with mixture of toluene (500 mL) and 1H,1H,2H,2H-perfluorooctyltriethoxysilane (2.5 g) has been performed; this mixture has been kept maximum 72 h under extractor hood at ambient temperature and then the powder was filtered and washed with pure toluene and finally was kept about 72 h under extractor hood for evaporating the toluene inside the powder. At the last, with the purpose of completely dry the powder, it was kept in an oven, maximum 4 h at 70°C.

By performing contact angle measurement, the wetting behavior of hydrophobic glass beads has been measured to verify whether the surface of glass beads was chemically modified. A mono-layer of hydrophobic glass beads has been prepared on a microscope slide then a droplet of water has been put over the sample. The contact angle has been measured based on taken images from sample and five replicates were performed for each sample, under ambient conditions. The

contact angle for hydrophobic glass beads was 142° ± 3°. This value was larger than 90° which is a confirmation of hydrophobic surface formulation.

2.2. GranuDrum/Rheometer

The GranuDrum is one of the most extensively used practical geometry to study the flow behavior of granular material [6, 33, 34, 35]; especially non cohesive powders [6]. GranuDrum evaluates the flow properties of powders in a free flowing regime and the only applied stress on the powders is due to their own weight [36, 37]. The experimental set up in this study presented in Figure 1, consists of a drum with two glass walls which rotates around its central axis with the angular velocity Ω. The flowing dynamics of powders inside the drum is function of this rotating angular velocity. The drum is generally half-filled with the powder whereas the length and the diameter of the drum are respectively 20 mm and 84 mm. During rotation, the drum is back lighted by using a stroboscope and a CCD camera takes pictures of powder-air interface position inside drum. For each imposed angular velocity, 50 pictures are taken, separated by 0.5 s. After monitoring the flow of powders via a camera then the images are processed by using image-processing algorithm. In the images, the granular material appears in black and the air appears in white, whereby an edge detection determines the position of the powder-air interface. From this analysis, two measurements are extracted: the average interface position and the fluctuations around this average position. Both of these measurements are calculated according to the average of 50 pictures that have been taken from powder-air interface inside rotating drum in each imposed angular velocity. Based on the average interface position, the flowing angle α_f is measured in the center of the flow which is the angle between the horizontal and the average interface. Also, the standard deviation calculated from the fluctuations of the powder-air interface, this parameter is called cohesive index σ_f and is directly linked to the cohesion inside drum. In fact, in the range of considered rotating speed, the cohesive granular material leads to irregular flow and non-cohesive granular material leads to a continuous flow. In this study, the rotating angular velocity has been selected between 2-30 rpm.

2.3. GranuPack

Measuring the tapped density and packing dynamic of powders is very popular in powder

characterization [6, 10]. The GranuPack equipment presented in Figure 2 developed to automate the procedure since it is usually realized with naked eyes. The analyzing cell is made of a tube of $D = 26$ mm in diameter and $L = 150$ mm in length. This tube is metallic to avoid the accumulation of electrostatic charges during measurement. A narrower and bottomless tube ($L = 170$ mm, $D_{inner} = 22.2$ mm and $D_{outer} = 25.4$ mm) is inserted into this measurement tube and filled with the powder to analyze. Afterward, it is slowly removed upward at the velocity $v = 1$ mm/s. This initialization procedure avoids human intervention and then increases the reproducibility.

A light hollow cylinder is placed on the top of the pile to keep it flat during the compaction process. The tube goes up and down over a height of $\Delta z = 3$ mm with the frequency $f = 1000$ ms in order to compact the granular pile. A distance sensor measures position of the hollow cylinder after each tap and computes the bulk volume V of the pile. As the introduced mass of powder is known, then the evolution of bulk density of powder ρ_b has been calculated as a function of tap number t. The bulk density is the ratio between mass m and volume V of the powder. The packing fraction η is calculated by dividing bulk density ρ_b by the true density of particles ρ_t. After recording packing fraction for each tap, compaction curve has been fitted with the classical logarithmic model [39],

$$\eta(t) = \eta_\infty - \frac{\eta_\infty - \eta_0}{1 + \ln(1 + t/\tau)} \quad (1)$$

Where, t is the number of tapes, the fitting parameters η_∞ & τ are asymptotic volume fraction and compaction characteristic time, respectively. The asymptotic volume fraction is representative of maximal packing fraction achieved by tapping the powders. With this parameter, one obtains the final packing fraction η_∞ consequently the more common parameter, Hausner ratio $\mathrm{Hr} = \frac{\eta_{500}}{\eta_0}$ [6, 40, 41]. The Hausner ratio is correlated to the powder flowability whereby high value of Hr corresponds to low flowability.

2.4. GranuCharge

Electrostatic charges are created due to the triboelectric effect inside a powder during a flow; meaning that the particles exchange charge at the result of contact with the other particles and

devices wall. Figure 3 illustrates GranuCharge equipment, it is a very useful equipment to measure the ability of a flowing powder to be charged electrostatically. It measures electrostatic charge of the powders by putting them in motion under the influence of gravity. In this measurement, the experimental set up consists of three parts: a stainless-steel pipe, a V-tube and a Faraday cup. The stainless-steel pipe is for feeding the V-tube by automatic rotation inside the tube.

In general, the material of the V-tube can be selected in the following list: stainless steel 316 L, aluminum 6063-T6, borosilicate glass, ABS, PVC and HDPE. The Stainless Steel 316 L was used in this study. The V-tube itself consists of two tubes with the length of L = 350 mm and diameter D = 47 mm; the two parts are connected together with the angle of 90°. After feeding the tube by a stainless-steel pipe the powders flow inside V-tube and at the end they fall into a faraday cup which is connected to an electrometer to measure the powders charge obtained during flow. Before starting each test, the whole assembly has been connected to the earth to be sure that they are discharged. The electrometer is capable of measuring charge ranging 0.1 nC - 1 µC. The powder charge density is computed by dividing calculated charge by the mass of powder. The charge density unit is Coulomb per kilogram. The powders can obtain negative or positive charge after flow, based on their tendency to obtain or lose electron [15].

2.5. Discovery HR3-Rheometer

The rheology of powders subject to vibration has been studied in this paper as well. With this objective, the Discovery HR3-rheometer has been implemented (see Figure 4). The implemented geometry in this study is a cylindrical baffle cell (radius = 25 mm, baffle height = 8.5 mm) with a four blades vane (radius = 7.5 mm, length = 51 mm). Only 21 mm of vane height has been immersed inside the powder. Indeed, in the case of immersing the whole vane inside the powder, the torque applied to shear the powder sample exceeds the limit of the apparatus. The utilized cell is similar to the cylindrical couette cell with the annular gap = 10 mm. The characterization cell is attached to a shaker at the bottom with the computer controlled sinusoidal transmitted vibration in close-loop system; detailed information can be found in [44, 45]. The mechanical vibrational stress corresponds to the sample vibrational energy which is defined as $\sigma_v = (1/2)\rho A^2(2\pi f)^2$, where ρ is the powder density, A is the vibration amplitude and f is the vibration frequency. The frequency and amplitude of vibration which has been used in this study is 60 Hz and 100 µm,

respectively. Pre-vibration has been applied at 70 Hz during 10 min for removing any packing history before each measurement. The volume fraction of glass beads is $\phi_{glass} \approx 0.61$ [45, 21] ($\rho_{glass} = 2500\ kg/m^3$). All tests have been carried out at imposed shear stress with the range of 4.5-188 Pa and the measured shear rate ranged as $3\times10^{-5} - 10 s^{-1}$.

2.6. Humid control

In this stage, the measurements were performed first with the GranuDrum and the GranuCharge with the objective of studying effect of humidity. The powder was placed in a rotating drum at 1 rpm with a controlled humid air flow during 1 h. As the powder was continuously mixed under drum rotation, the humidity absorption is assumed to be sufficient to observe changes in powder behavior. With this method, the accessible range for humidity is $RH = 35 - 95\% \pm 5\%$ inside the drum.

On the other side, another methodology has been utilized for the humid control of powders. In this case, the powder has been kept in a humid chamber longer to ensure absorption of enough humidity. With this purpose, the sufficient range of humid control time has been reported to be two days as minimum and one week as maximum storage time in a humid chamber for glass beads [46, 47]. According to the literature the powder behavior has the same trend in both storage times. Therefore, here in our study each powder sample has been kept 72 h in a humid chamber and the range of imposed humid value was between 35 % up to 90 % at 20°C. The relative humidity of powders has been confirmed by using TH200 thermoconstanter(Novasina, Switzerland) at a temperature of 25°C; after taking them from the humid chamber. This apparatus has a measuring range comprised between 0.05 to 1.00 and an accuracy of ± 0.01 over a temperature range between 0 and 50°C. More precisely, 1 g sample is introduced into a polypropylene cup deposited in the sealed enclosure of the apparatus. The free water moistens or dries the air inside the enclosure until the balance is reached. The relative humidity has been measured using an electrolytic sensor. After humid control then the powder characterization has been done by Discovery HR3-Rheometer under vibration.

3. Results

3.1. Influence of surface treatment

3.1.1. Flowability

In the literature, a vast body of researches conducted to study the powder flow behavior by different shear cell tests [48, 49, 50, 51, 52, 53]. In our previous study we studied flowability of raw and hydrophobic glass beads with shear cell [31]. For this measurement, FT4 powder rheometer was utilized to evaluate powder flow at high shear rate by rotating shear head. In this measurement, first the powder was preconsolidated at 9 kPa normal stress. Then, decreasing normal stresses from 7 to 3 kPa by 1 kPa steps were successively applied and the shear stresses (τ) (s) required to make the powder flow (i.e. to induce preconsolidated powder bed failure) were recorded. (see Figure 5). In our measurements, the yield locus presented the same values for both powders over the entire range of normal stress showing similar flow behavior in raw and hydrophobic glass beads.

In addition, the flowing factor ff characterizes powder flowability in this measurement. This factor is calculated by yield locus approach of software, whereby major principal stress (σ_1) and unconfined yield strength (σ_c) dedicated based on yield locus approach ($ff = \sigma_1 / \sigma_c$). The flowing factor has been recorded as 19.70 ± 0.81 and 19.74 ± 1.66 for raw and hydrophobic glass beads, respectively.

According to the Jenike classification [54], powders are considered as not flowing for $ff < 1$, very cohesive for $1 < ff < 2$, cohesive for $2 < ff < 4$, easy-flowing for $4 < ff < 10$ and free-flowing for $ff > 10$. Therefore, based on this criteria our powders fall into category of free-flowing powders with the same flowability at high shear rate condition.

3.1.2. Charge

The electrostatic charge measurement of raw and hydrophobic glass beads has been performed with the GranuCharge equipment with the humidity and temperature range at 37-44 % and 22°C, respectively. Figure 6 represents the results corresponding to this test. Three values have been collected for each sample. These values include initial charge q_0, final charge q_f and $\Delta q = q_f - q_0$. The initial charge was measured before performing the test by directly introducing the powder inside Faraday cup and final charge is a measurement after powder flow through the V-tube. The obtained results show that both powders had almost zero initial electrostatic charge. After flow

inside stainless steel V-tube, the raw glass beads kept this tendency for having almost zero charge however hydrophobic glass beads obtained a negative charge. The quantity of each sample was 50 mL during measurement.

3.1.3. Cohesion

Figure 7 shows the evolution of the cohesion σ_f and the flowing angle α_f of raw and hydrophobic glass beads. It has been observed that cohesion of both samples have been enhanced by increasing the rotating speed of the drum, meaning that their flowability decreases under motion, particularly after 10 rpm. Hydrophobic glass beads showed slightly more cohesion than raw glass beads. This could be explained by the GranuCharge measurements where hydrophobic glass beads presented more electrostatic charge than raw glass beads. This can lead to higher cohesion of hydrophobic glass beads under motion (see Figure 6).

3.1.4. Packing dynamics

The compaction curves of raw and hydrophobic glass beads have been recorded with the GranuPack in standard conditions of temperature and pressure and they have been presented in Figure 8. One observes the difference of density between two powders at the beginning and at the end of the compaction process. In addition, Figure 9 presents the Hausner ratio H_r where the packing density before tapping η_0, after 500 tap η_{500} and the asymptotic packing fraction after an infinite number of tap η_∞ obtained from the equation (1). One observes a slightly higher Hausner ratio for the hydrophobic glass beads than for the raw glass beads. This can be related to the cohesion since high Hausner ratio generally corresponds to poor flowability and therefore high cohesion. Also, the slight density difference of powders can be due to the different rearrangements of particles during measurement.

3.2. Impact of humidity

Influence of humidity on flowability of raw and hydrophobic glass beads has been studied. Indeed, it has been reported that humidity can change the charging of a powder [15] whereby it can induce variation of cohesion and consequently it modifies powder flowability. We implemented GranuDrum with the speed of 4 rpm at standard conditions and GranuCharge equipments to

measure powders cohesion and electrostatic charge under influence of humidity. Here, the humid control has been done with a rotating drum with humid-air controlled flow. The powders have been kept shortly 1 h in each selected humid range, the accessible range for humidity is $RH = 35 - 95\% \pm 5\%$ inside the drum.

Figure 10 shows evolution of the cohesive index of raw and hydrophobic glass beads inside GranuDrum after humid control. The cohesive index of raw glass beads has been increased after 80 % RH which shows high sensitivity of raw glass beads to the humidity after this value of humidity. However, the cohesive index of hydrophobic glass beads had almost constant value in all range of humid control, showing less sensitivity of this powder to the humidity. In addition, based on Figure 11, we have seen that control glass beads have almost zero electrostatic charges in all ranges of humid control. While the electrostatic charge of hydrophobic glass beads decreased by increasing the humidity up to 80 % of humidity and after this range of humidity hydrophobic glass beads lost their electrostatic charge completely. Therefore, we have observed that the powder cohesion and electrostatic charge can evolve by humidity in spite of short humid control time. As a complementary test, the evolution of viscosity of our two formulations have been considered with Discovery HR3-Rheometer Discovery at low shear rate condition (Figure 4). In this case, the powders humidity has been controlled longer during 72 h before each measurement in a humid chamber; then the rheological measurements have been done in an experimental room in ambient temperature and the humidity of room was not controlled during measurements.

Figure 12 presents evolution of the viscosity of raw and hydrophobic glass beads as a function of humidity at 35-90 % RH; the figure has been plotted in given shear rate at $\gamma = 5*10^{-5} s^{-1}$. Based on viscosity curves, the hydrophobic glass beads presented higher viscosity than raw glass beads. This can be due to the fact that hydrophobic glass beads presented more electrostatic charge than raw glass beads in the humid range of 35-80 % (see Figure 11). In addition, the viscosity curve of hydrophobic glass beads stayed always constant even after 80 % of humidity. This is due to the tendency of hydrophobic glass beads to repel water even at 90 % of humidity. By taking into account that the rheological measurements have been done in a dry room, then a slight amount of presented water in high humidity range on hydrophobic glass beads surface evaporated rapidly due to the tendency of this powder to repel the water. The rheological measurement time was between 20-30 min which was enough for evaporating the slight surface water and getting the powder recharged again. It should be indicated that the charge measurement

time in Figure 11 which has been done with GranuCharge was a few seconds, meaning that the powders did not have enough time to recharge.

In general, raw glass beads showed lower viscosity than the hydrophobic glass beads which can be due to the lower electrostatic charge of raw glass beads compared to hydrophobic glass beads. However, after 80 % of humidity the viscosity of raw glass increased dramatically which is due to the sensitivity of raw glass beads to humidity that resulted in high cohesion. In addition, this increasing shift of viscosity of raw glass beads can be due to the condensation effect, however for the hydrophobic glass beads the viscosity was constant throughout the same range of humidity. It indicates that performing hydrophobic surface treatment on glass beads decreases the sensitivity of glass beads to the humidity therefore the viscosity of hydrophobic glass beads stayed constant in all range of humidity. In order to check the stability of hydrophobic surface formulation on glass beads, the contact angle measurement performed at the end of measurements performed by Discovery HR3-rheometer (the longest test in this paper). Hydrophobic glass beads presented the same water contact angle than before performing any test.

4. Discussion

The FT4 shear cell test results from our previous study [31] reported the same flowability for raw and hydrophobic glass beads at high shear rate condition. Whereby, these two powders classified as easy flowing powders based on Jenike classification [54]. These results are in agreement with the similar study performed on raw glass beads by modified shear apparatus [55], where dry raw glass beads recorded as no cohesive powder. In addition, they reported that the value of consolidation stress during measurement had no significant influence on the shear data [50, 55]. According to the literature, the powder flowability was expected to increases when increasing particle size [31, 56, 57]. In fact, surface area to volume ratio decreases with increasing size which results in better flowability of large size powders.

In addition, based on GranuPack results one observes a small difference in cohesion between the two powders which is also observed with the Hausner ratio. Indeed a high Hausner ratio generally corresponds to a high cohesion. However this difference was not significant enough to observe a change in flowability as showed in Figure 5. It should be mentioned that slightly higher value of the density in hydrophobic glass beads can be due to the different rearrangements

of particles in this case.

According to the GranuDrum measurement, the powders cohesion was increasing by increasing speed of drum. This can be due to an internal effect such as more electrostatic charge exchange because of more contact time of particles inside drum. To verify this hypothesis the cohesion measurement has been done with GranuDrum at the speed of 30 rpm with two different conditioning rotating times: 15 sec as short rotating time and 30 min as long rotating time. The measurement has been performed as usual with 50 pictures separated by 0.5 s. As illustrated in Figure 13, it has been observed that the value of cohesion is higher when the rotating time is longer (30 min). As explained already, this is due to the more charge exchange coming from more contact time, which it results in increasing electrostatic charge.

Discovery HR3-rheometer collected the data corresponding to vibrational rheology of powders after humid control. It has been observed that hydrophobic glass beads have higher viscosity than raw glass beads, which is consistent with the observations of the cohesion and the Hausner ratio. It has been reported that silanization (hydrophobic surface formulation) increases powder electrostatic charge [58] and consequently cohesion [59]. Here, hydrophobic glass beads presented more electrostatic charge than raw glass beads before applying vibration, therefore applying vibration induced building up more electrostatic charge consequently higher viscosity has been recorded for hydrophobic glass beads. Based on literature, the particle electrostatic charge is in inverse relation with particles size, whereby by decreasing particles size the electrostatic charge per unit area increases which is due to the more specific surface area in small size particles compared to large particles [19]. Furthermore, according to the collected data with Discovery HR3-rheometer, we have seen that hydrophobic treatment decreases sensitivity of glass beads to the humidity since after 80% of humidity raw glass beads presented an impressive increase in the viscosity while viscosity of hydrophobic surface treated glass beads had almost constant value from the beginning up to end of humid control. This tendency of hydrophobic glass beads has been recorded with AFM measurement on single hydrophobic glass beads over the same range of humidity in the literature [27]. In our case, we collected the bulk behavior of hydrophobic glass beads over large relative humidity range which confirms the last findings on single hydrophobic glass beads [27]. In addition, it should be indicated that based on literature was found that there is a critical relative humidity at which the raw glass beads undergoes a transition from free-flowing to stick–slip behavior [26]. In our study, this critical value of humidity seems to be

after 70% of relative humidity where raw glass beads presented a viscosity shift, this value is in agreement with the literature. In addition, this critical humidity increases with increasing particle size [26]. At the end of measurements performed by Discovery HR3-rheometer (the most longest test in this paper) the contact angle measurement performed on hydrophobic glass beads with the objective of checking the stability of hydrophobic surface formulation on glass beads. Hydrophobic glass beads presented the same water contact angle than before performing any test. In the following the collected raw data from different set of measurements have been presented in table 1.

5. Conclusion

This paper presented a study on flow behavior of raw and hydrophobic surface formulated glass beads. The objective was to evaluate the influence of hydrophobic surface treatment on glass beads as well as influence of humidity on flow behavior of raw and hydrophobic glass beads. With this objective, we considered our powders flow behavior under different processing dynamics to collect the essential factors and indices describing the behavior of a powder. Based on shear cell measurement, the powders reported similar flowability. However, GranuCharge measurement presented a charge difference between hydrophobic and raw glass beads. It reported negative charge for hydrophobic glass beads and almost zero charge for raw glass beads which was expected to influence the powders flow behavior. This difference in charge could explain the slight difference in the Hausner ratio and cohesion. This issue has been confirmed with the cohesive index values measured by GranuDrum, the hydrophobic glass beads presented higher cohesion under rotation with GranuDrum which was indicative of decreasing flowability of hydrophobic glass beads under motion due to the tendency of this powder to build up electrostatic charge. In addition, the influence of air humidity on utilized powders has been studied with Discovery HR3-rheometer at low shear rate condition. The obtained results evidenced that under vibrational rheology the hydrophobic glass beads is less flowable than raw glass beads. It was because under vibration the electrostatic charge built up by hydrophobic glass beads that it was resulted in higher viscosity in this power. At high shear rate condition with shear cell test, both powders presented same flowability while at low shear rate condition with HR3-rheometer the raw glass beads showed lower flowability. This is because at high shear rate the powders are in frictional regime

meaning that the friction between particle-particle governs the power flowability. Since raw and hydrophobic glass beads had similar surface properties therefore similar flowability has been recorded for them at frictional regime; however at low shear rate condition the flowability of powders are linked to their surface cohesion where the hydrophobic glass beads with more surface cohesion (due to the electrostatic charge) presented high viscosity. Furthermore, it has observed that by doing hydrophobic treatment on raw glass beads the sensitivity of powder to the humidity decreases, whereby even at high range of humidity it kept its flowability as in low humidity range. However, raw glass beads lost their flowability dramatically at higher value of humidity.

Acknowledgments – This study is conducted in the framework of the "PowderReg" project, funded by the European program Interreg VA GR within the priority axis 4 "Strengthen the competitiveness and the attractiveness of the Grande Région / Gro β region".

Credit Author Statement
Shirin Enferard : Conceptualization, Investigation, Methodology, Writing - Original Draft, Formal analysis
Salvatore Pillitteri : Investigation, Writing - Original Draft
Geoffroy Lumay : Formal analysis
Claire Gaiani : Supervision
Sebastien Kiesgen De Richter : Project administration, Funding acquisition
Michaël Marck : Resources
Syrym Umbetov : Investigation
Nicolas Vandewalle : Writing - Review & Editing
Mathieu Jenny : Conceptualization, Supervision

Declaration of interests
The authors declare that they have no known competing financial interests or personal relationships that could have appeared to influence the work reported in this paper.

References

[1] E. Guerin, P. Tchoreloff, B. Leclerc, D. Tanguy, M. Deleuil, G. Couarraze, *Rheological characterization of pharmaceutical powders using tap testing, shear cell and mercury porosimeter*, International journal of pharmaceutics **189(1)**, 91-103 (1999).

[2] J. Xiang, L. Liu, X. Cui, Y. He, G. Zheng, C. Shi, *Effect of Fuller-fine sand on rheological, drying shrinkage, and microstructural properties of metakaolin-based geopolymer grouting materials*, Cement and Concrete Composites **104**, 103381 (2019).

[3] JA. Grabowski, V-D. Truong, CR. Daubert, *Nutritional and rheological characterization*

of spray dried sweetpotato powder, LWT-Food Science and Technology **41(2)**, 206-216 (2008).

[4] P. Coussot, *Rheometry of pastes, suspensions, and powders: applications in industry and environment*, John Wiley & Sons (2005).

[5] C. Salameh, J. Scher, J. Petit, C. Gaiani, C. Hosri, S. Banon, *Physico-chemical and rheological properties of Lebanese kishk powder, a dried fermented milk-cereal mixture*, Powder technology **292**, 307-313 (2016).

[6] G. Lumay, F. Boschini, K. Traina, S. Bontempi, J.-C. Remy, R. Cloots and N. Vandewalle, *Measuring the flowing properties of powders and grains*, Powder technology **224**, 19-27 (2012).

[7] U.V. Shah, V. Karde, C. Ghoroi, J.YY. Heng, *Influence of particle properties on powder bulk behaviour and processability*, Powder technology **518(1-2)**, 138-154 (2017).

[8] A. Castellanos, *The relationship between attractive interparticle forces and bulk behavior in dry and uncharged fine powders*, Advances in physics **54(4)**, 263-376 (2005).

[9] AM. Stoklosa, RA. Lipasek, LS. Taylor, LJ. Mauer, *Effects of storage conditions, formulation, and particle size on moisture sorption and flowability of powders: A study of deliquescent ingredient blends*, Food research international **49(2)**, 783-791 (2012).

[10] European pharmacopoeia 7.0, Powder flow Chapter **2.9.36**, 308 (2010).

[11] R. L. Carr, *Evaluating flow properties of solids*, Chemical engineering **72**, 163-168 (1965).

[12] H. Hausner, *Friction conditions in a mass of metal powder*, Int. J. Powder Metall **3**, 7-13 (1967).

[13] S. Wang, Z. Yunlong, Y. s. Zhou, S. Li, F. Fan, L. Lin, Z. L. Wang, *Molecular surface functionalization to enhance the power output of triboelectric nanogenerators*, Journal of Materials Chemistry A **4(10)**, 3728-3734 (2016).

[14] F. Fulchini, U. Zafar, C. Hare, M. Ghadiri, H. Tantawy, H. Ahmadian, M. Poletto, *Relationship between surface area coverage of flow-aids and flowability of cohesive particles*, Powder Technology **322**, 417-427 (2017).

[15] A. Rescaglio, J. Schockmel, N. Vandewalle and G. Lumay, *Combined effect of moisture and electrostatic charges on powder flow*, EPJ Web of Conferences **140**, EDP Sciences 13009 (2017).

[16] E. Mersch, G. Lumay, F. Boschini, S. Bontempi, N. Vandewalle, *Effect of an electric field*

on an intermittent granular flow, Physical Review E **81(4)**,0413097 (2010).

[17] DA. Hays, J. Mason, PJ. Mason, RE. Zeman, D.Jackson, *Fabrication of 3d objects via electrostatic powder deposition*, US Patent App.15/050,729 (2016).

[18] T. Stichel, T. Brandl, T. Hauser, B. Geißler, S. Roth, *Electrophotographic multi-material powder deposition for additive manufacturing*, Procedia CIRP **74(3)**, 249-253 (2018).

[19] U. Zafar, F. Alfano, M. Ghadiri, *Evaluation of a new dispersion technique for assessing triboelectric charging of powders*, International journal of pharmaceutics **543(1-2)**, 151-159 (2018).

[20] E. M. Sloot, N. P. Kruyt, *Theoretical and experimental study of the transport of powders by inclined vibratory conveyors*, Powder technology **87(3)**, 203-210 (1996).

[21] N. Gaudel, S. Kiesgen De Richter, N. Louvet, M. Jenny and S. Skali-Lami, *Bulk and local rheology in a dense and vibrated granular suspension*, Physical review E **96(6)**, 062905 (2017).

[22] G. Lumay, K. Traina, F. Boschini, V. Delaval, A. Rescaglio, R. Cloots and N. Vandewalle, *Effect of relative air humidity on the flowability of lactose powders*, J. Drug Deliv. Sci. Technol. **35**, 207-212 (2016).

[23] N. Vandewalle, G. Lumay, F. Ludewig, J. E. Fiscina, *How relative humidity affects random packing experiments*, Phys. Rev. E. **85(3)**, 031309 (2012).

[24] J. E. Fiscina, G. Lumay, F. Ludewig and N. Vandewalle, *The compaction dynamics of wet granular assemblies*, Phys. Rev. Lett.**105(4)**, 048001 (2010).

[25] M. J. Colbert, M. Grandbois, N. Abatzoglou, *Identification of inter-particular forces by atomic force microscopy and how they relate to powder rheological properties measured in shearing tests*, Powder Technology **284**, **396-402**, (2015).

[26] A. J. Forsyth, S. Hutton, M. J. Martin, *Effect of cohesive interparticle force on the flow characteristics of granular material*, Powder Technology **126(2)**, **150-154**, (2002).

[27] R. Jones, H. M. Pollock, J. AS. Cleaver, C. S. Hodges, *Adhesion forces between glass and silicon surfaces in air studied by AFM: Effects of relative humidity, particle size, roughness, and surface treatment*, Langmuir **18(21)**, **8045-8055**, (2002).

[28] G. Landi, D. Barletta, P. Lettieri, P. Massimo, *Flow properties of moisturized powders in a Couette fluidized bed rheometer*, International Journal of Chemical Reactor Engineering **10(1)**, **8045-8055**, (2012).

[29] G. Landi, D. Barletta, P. Massimo, *Modelling and experiments on the effect of air humidity on the flow properties of glass powders*, Powder technology **207(1-3)**, **437-443**, (2011).

[30] E. Teunou, JJ. Fitzpatrick, *Effect of relative humidity and temperature on food powder flowability*, Journal of Food Engineering **42(2)**, **109-116**, (1999).

[31] S. Enferad, J. Petit, C. Gaiani, V. Falk, J. Burgain, S. Kiesgen De Richter and M. Jenny, *Effect of particle size and formulation on powder rheology*, Particulate Science and Technology **1-9**, (2020).

[32] Z. Kutelova, H. Mainka, K. Mader-Arndt, W. Hintz and J. Tomas, *Functionalization and surface modification of spherical glass beads*, 7th International Conference for Conveying and Handling of Particulate Solids, Friedrichshafen, Germany (2011).

[33] N. Taberlet, R. Patrick and E.J. Hinch, *S shape of a granular pile in a rotating drum*, Physical Review E **73(5)**, 050301 (2006).

[34] X. Y. Liu, E. Specht and J. Mellmann, *Experimental study of the lower and upper angles of repose of powders in rotating drums*, Powder Technology **154(2-3)**, 125-131 (2005).

[35] J. Rajchenbach, *Flow in powders: From discrete avalanches to continuous regime*, Physical Review Letters **65(18)**, 2221 (1990).

[36] H. H. Hausner, *Friction conditions in a mass of metal powder.*, Polytechnic Inst. of Brooklyn. Univ. of California, Los Angeles (1967).

[37] S. Chikosha, TC. Shabalala, HK. Chikwanda *Effect of particle morphology and size on roll compaction of Ti-based powders*, Powder technology **264**, 310-319 (2014).

[38] G. Lumay, F. Boschini, K. Traina, S. Bontempi, J-C. Remy, R. Cloots, N. Vandewalle, *Measuring the flowing properties of powders and grains*, Powder technology **224**, 19-27 (2012).

[39] J. B. Knight, C. G. Fandrich, C. N. Lau, H. M. Jaeger & S. R. Nagel, *Density relaxation in a vibrated granular material*, Phys. Rev. E **51(5)**, 3957-3963 (1995).

[40] K. Traina, R. Cloots, S. Bontempi, G. Lumay, N. Vandewalle & F. Boschini, *Flow abilities of powders and powders evidenced from dynamical tap density measurement*, Powder Technology **235**, 842-852 (2013).

[41] A. Saker, M. G. Cares-Pacheco, P. Marchal and V. Falk, *Powders flowability assessment in granular compaction: What about the consistency of Hausner ratio?*, Powder Technology. **354**, 52-63 (2019).

[42] A. Rescaglio, F. De Smet, A. Luc and G. Lumay, *Tribo-electrification of pharmaceutical powder blends*, Particulate Science and Technology. (2019).

[43] N. Gaudel, *Rhéologie et contrôle des écoulements de dispersions granulaires par l'application de vibrations*, PhD thesis, Université de Lorraine, 198301 (2018).

[44] Ph. marchal, N. Smirani and L. Choplin, *Rheology of dense-phase vibrated powders and molecular analogies*, Journal of rheology **53(1)**, 1-29 (2009).

[45] C. hanotin, S. Kiesgen De Richter, Ph. Marchal, L. J. Michot and C. Baravian, *Vibration-induced liquefaction of granular suspensions*, Physical review letters **108(19)**, 198301 (2012).

[46] L. Oger, C. El Tannoury, R. Delannay, Y. Le Gonidec, I. Ippolito, Y. Roht, I. Gómez-Arriaran, *Effect of grain size and material on humid granular avalanche events*, Bulletin No. 123 of the Utah Engineering Experiment Station, hal-01825012v2 (2018).

[47] L. Oger, C. El Tannoury, R. Delannay, Y. Le Gonidec, I. Ippolito, Y. L. Roht, I. Gómez-Arriaran, *Dynamic behavior of humid granular avalanches: Optical measurements to characterize the precursor activity*, Physical Review E **101(2)**, 022902 (2020).

textcolorred

[48] A. Angus, L.A.A. Yahia, R. Maione, M. Khala, C. Hare, A. Ozel, R. Ocone, *Calibrating friction coefficients in discrete element method simulations with shear-cell experiments*, Powder Technology **372**, **290-304**, (2020).

[49] M. Lupo, D. Schütz, R. Maione, E. Riedl, D. Barletta, M. Poletto, *Assessment of a powder rheometer equipped with a cylindrical impeller for the measurement of powder flow properties at low consolidation*, Powder Technology **357**, **281-290**, (2019).

[50] L.A.A. Yahia, T.M. Piepke, R. Barrett, A. Ozel, R. Ocone ütz, R. Maione, E. Riedl, D. Barletta, M. Poletto, *Development of a virtual Couette rheometer for aerated granular material*, AIChE Journal **66(6)**, **e16945**, (2020).

[51] K. Saleh, M.T.M. Abou Jaoude, M. Morgeneyer, E. Lefrancois, O. Le Bihan, J. Bouillard, *Dust generation from powders: A characterization test based on stirred fluidization*, Powder technology **255**, **141-148**, (2014).

[52] I. Tomasetta, D. Barletta, P. Lettieri, M. Poletto, *The measurement of powder flow properties with a mechanically stirred aerated bed*, Chemical engineering science **69(1)**,

373-381, (2012).

[53] V. Francia, L.A.A. Yahia, R. Ocone, A. Ozel, *From Quasi-static to Intermediate Regimes in Shear Cell Devices: Theory and Characterisation*, KONA Powder and Particle Journal, **2021018**, (2021).

[54] A. W. Jenike, *Storage and flow of solids*, Bulletin No. 123 of the Utah Engineering Experiment Station **53**, No. 26, November 1964 (1976).

[55] P. Pierrat, D. K. Agrawal, H. S. Caram, *Effect of moisture on the yield locus of granular materials: theory of shift*, Powder Technology **99(3)** 220-227 (1998).

[56] KK. Lam, JM. Newton, *Influence of particle size on the adhesion behaviour of powders, after application of an initial press-on force*, Powder Technology **73(2)** 117-1257 (1992).

[57] S. Enferad, *Compactage et vieillissement des poudres: influence de la formulation*, PhD thesis, Université de Lorraine (2020).

[58] K.W. Biegaj, M.G. Rowland, T.M. Lukas, J. YY. Heng, *Surface chemistry and humidity in powder electrostatics: A comparative study between tribocharging and corona discharge*, Acs Omega **2(4)** 1576-1582 (2017).

[59] A. Hassanpour, M. Ghadiri, *Characterisation of flowability of loosely compacted cohesive powders by indentation*, Particle & Particle Systems Characterization **24(2)** 117-123 (2007).

Figure 1: Sketch of the GranuDrum equipment [38]. A cylinder is half-filled with the powder and rotates around its axis. For each rotating speed, a CCD camera takes 50 successive images of the flow. A dedicated algorithm enables to measure the flowing angle α_f and the fluctuations σ_f of the flow from the shape of the powder-air interface.

Figure 2: Sketch of the GranuPack equipment [38]. The powder is placed in a metallic tube and a light hollow cylinder is placed on the top of the pile to keep it flat during the compaction process. The taps correspond to successive free falls of the tube over a distance ΔZ. After each tap, the height h of the pile is measured. Finally, a compaction curve is obtained.

Figure 3: Left: Sketch of the GranuCharge which is used to measure the electrostatic charge created inside a powder after flow in contact with a selected material. Right: Picture of the powder

flowing from the tube 2 into the Faraday Cup measuring the electrostatic charge [42].

Figure 4: (a) Rheometer discovery (b) Schematics of couette type cell connected to shaker [45].

Figure 5: Flow parameters derived from shear cell test for raw and hydrophobic glass beads [31]. Each test has been repeated three times and the measurements have been done in ambient temperature. Error bars represent standard errors; they are not visible as their size are inferior to the marker size.

Figure 6: Evolution of the electrostatic charge of raw and hydrophobic glass beads. q_0 is initial electrostatic charge before flow, q_f is the final electrostatic charge after powder flow inside V-tube and Δq is the difference between the initial and the final charge. Error bars represent standard errors (corresponding to three repeated measurements); some were not visible as their size was inferior to the marker size. The measurement performed by the GranuCharge equipment. The humidity and temperature range are 37-44 % and 22°C, respectively.

Figure 7: Evolution of the flowing angle and cohesion of raw and hydrophobic glass beads under different rotational speed with the measurements performed by GranuDrum. Error bars represent standard errors (corresponding to three repeated measurements); some were not visible as their size was inferior to the marker size. The humidity and temperature range are 37-44 % and 22°C, respectively.

Figure 8: Experimental compaction curves for respectively raw glass beads, represented by grey squares, and hydrophobic glass beads, represented by orange dots. Both curves have been fitted with the logarithmic model (Eq.1), represented by plain curves of the same color, in order to obtain the typical compaction time and the asymptotic packing fraction after an infinite number of tap. The humidity and temperature range are 37-44 % and 22°C, respectively.

Figure 9: Comparison between the Hausner ratio $Hr = \frac{\eta_{500}}{\eta_0}$ of raw glass beads, in grey, and hydrophobic glass beads, in orange. Error bars represent standard errors (corresponding to three

repeated measurements).

Figure 10: Evolution of the cohesive index of raw and hydrophobic glass beads under humid control from 35% to 95% $\pm 5\,\%$. Error bars represent standard errors (correspond to three repeat of measurement); some were not visible as their size was inferior to the marker size. Both supplementary points out of the lines represent data from normal environmental conditions.

Figure 11: Evolution of the charge difference of raw and hydrophobic glass beads under humid control from 35% to 95% $\pm 5\%$. Error bars represent standard errors (corresponding to three repeated measurements); some were not visible as their size was inferior to the marker size. Both supplementary points out of the lines represent data from normal environmental conditions.

Figure 12: Evolution of the viscosity of raw and hydrophobic glass beads under humid control from 35% to 90%. The measurement has been done with Discovery HR3-rheometer under vibration and the figure has been plotted in a given shear rate $\gamma = 5*10^{-5} s^{-1}$.

Figure 13: Evolution of the cohesive index of raw and hydrophobic glass beads as a function of rotating time in GranuDrum. The rotating speed of drum was 30 rpm, error bars represent standard errors (corresponding to three repeated measurements). The humidity and temperature range are 37-44 % and 22°C, respectively.

Table 1: Recapitulation of the different values measured with the set of instruments; the humidity and temperature range are 37-44 % and 22°C, respectively. σ_f and α_f are correspond to the Figure 7.

Measures	Raw glass beads	Hydrophobic glass beads
ff (-)	19.70 ± 0.81	19.74 ± 1.66
Δ q (nC/g)	-0.30 ± 0.01	-4.55 ± 0.12
σ_f (a.u.) (30 rpm)	10.46 ± 0.21	13.80 ± 0.43
α_f (a.u.) (30 rpm)	39.73 ± 0.10	48.13 ± 3.43
η_0 (a.u.)	0.58 ± 0.01	0.59 ± 0.01

η_{500} (a.u.)	0.62 ± 0.01	0.64 ± 0.01
η_{∞} (a.u.)	0.63 ± 0.01	0.66 ± 0.01
Hr (a.u.)	1.06 ± 0.01	1.07 ± 0.01

Graphical abstract

Highlights

- At high shear rate, raw and hydrophobic glass beads had similar flowability.
- At low shear rate, hydrophobic glass beads were less flowable than raw glass beads.
- Hydrophobic formulation decreased sensitivity of glass beads to the humidity.
- Hydrophobic formulation increased the electrostatic charge of glass beads.

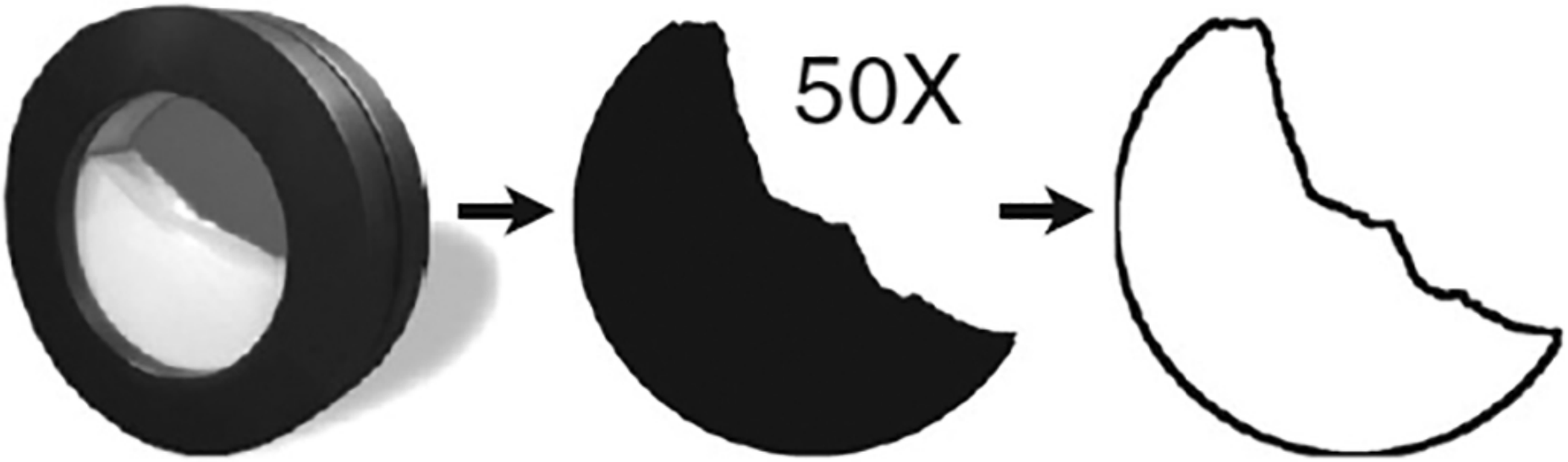

Figure 1

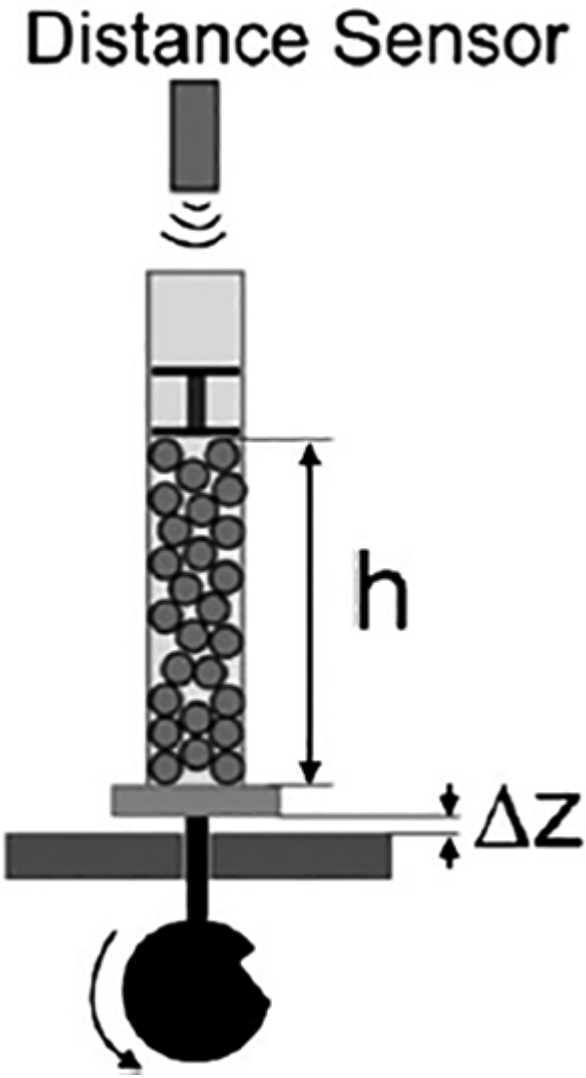

Figure 2

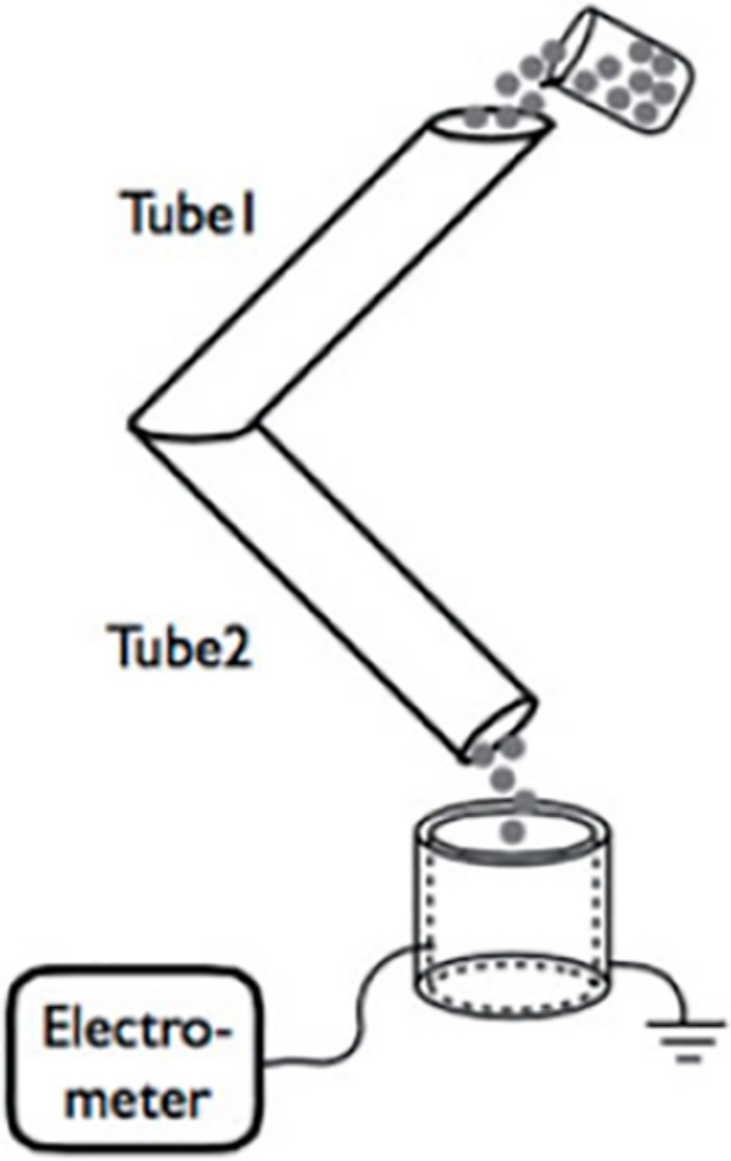

Figure 3

1. Rheometer « Discovery HR3 »
2. Measurement cell
3. Vane axis
4. Vibrator base

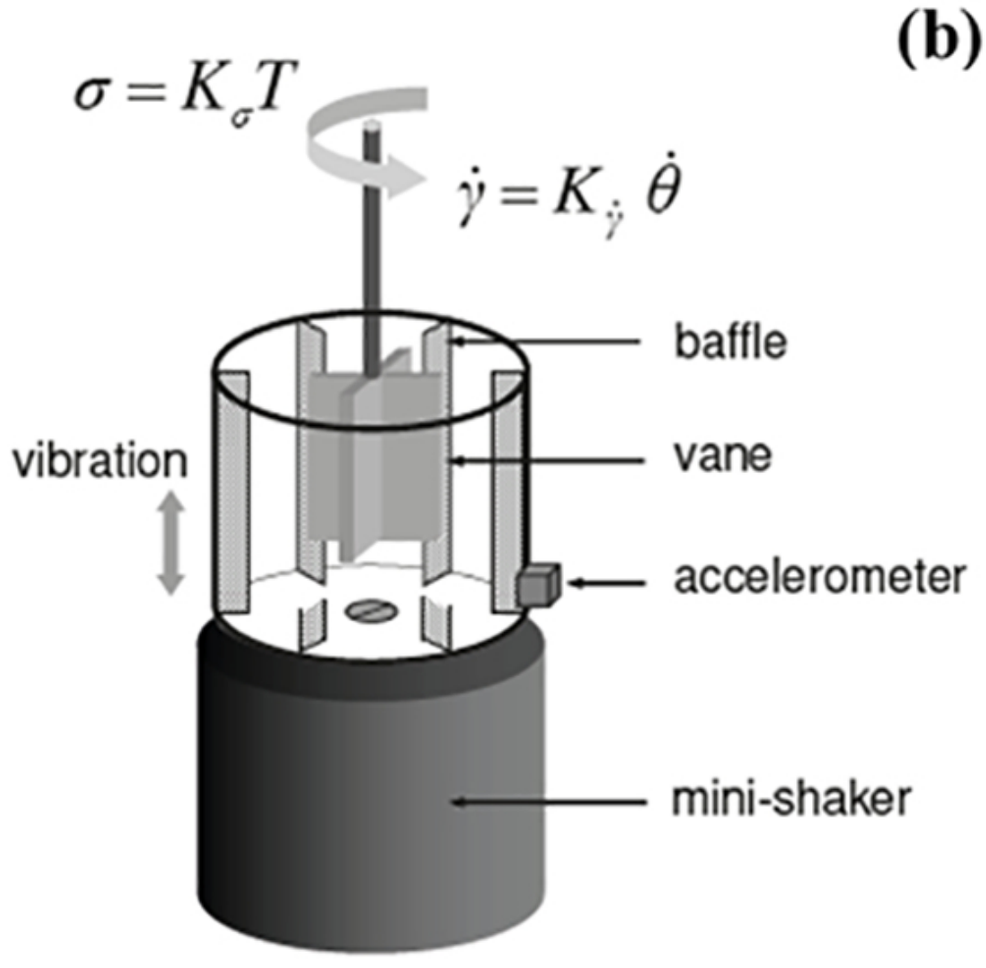

Figure 4

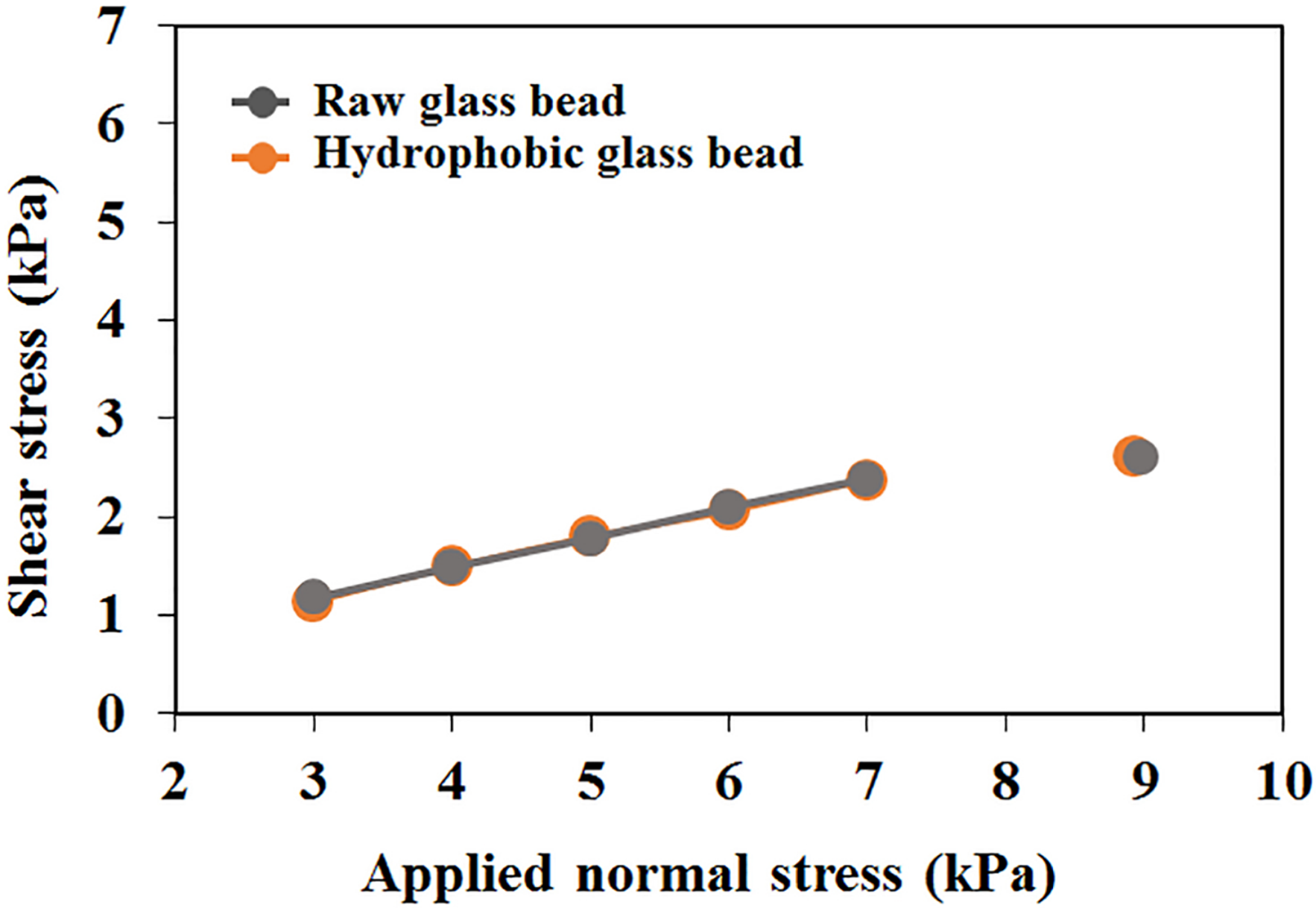
Raw glass bead
Hydrophobic glass bead
Shear stress (kPa)
Applied normal stress (kPa)
0
1
2
3
4
5
6
7
2
3
4
5
6
7
8
9
10

Figure 5

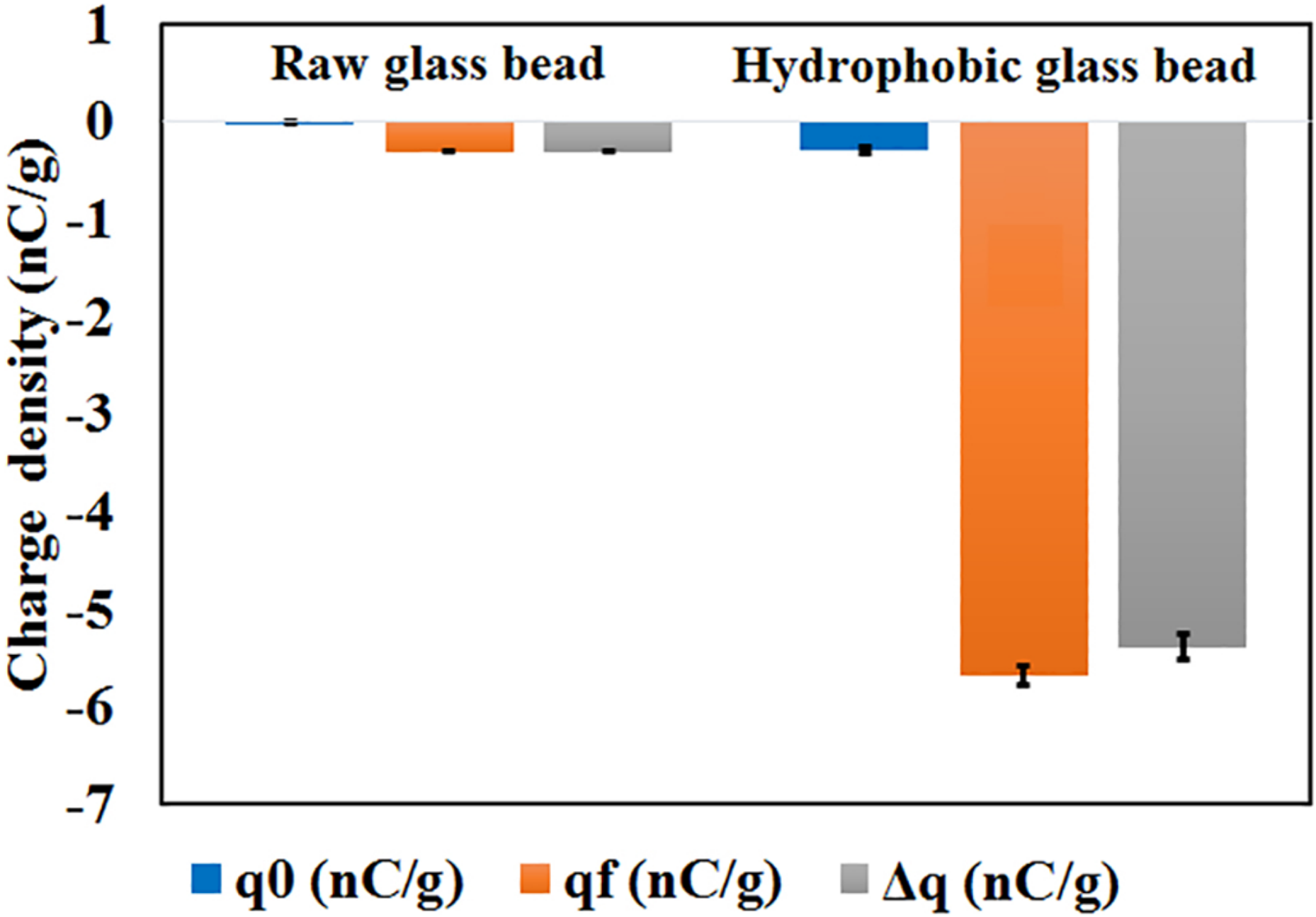
Raw glass bead
Hydrophobic glass bead
Charge density (nC/g)
1
0
-1
-2
-3
-4
-5
-6
-7
q0 (nC/g)
qf (nC/g)
Δq (nC/g)

Figure 6

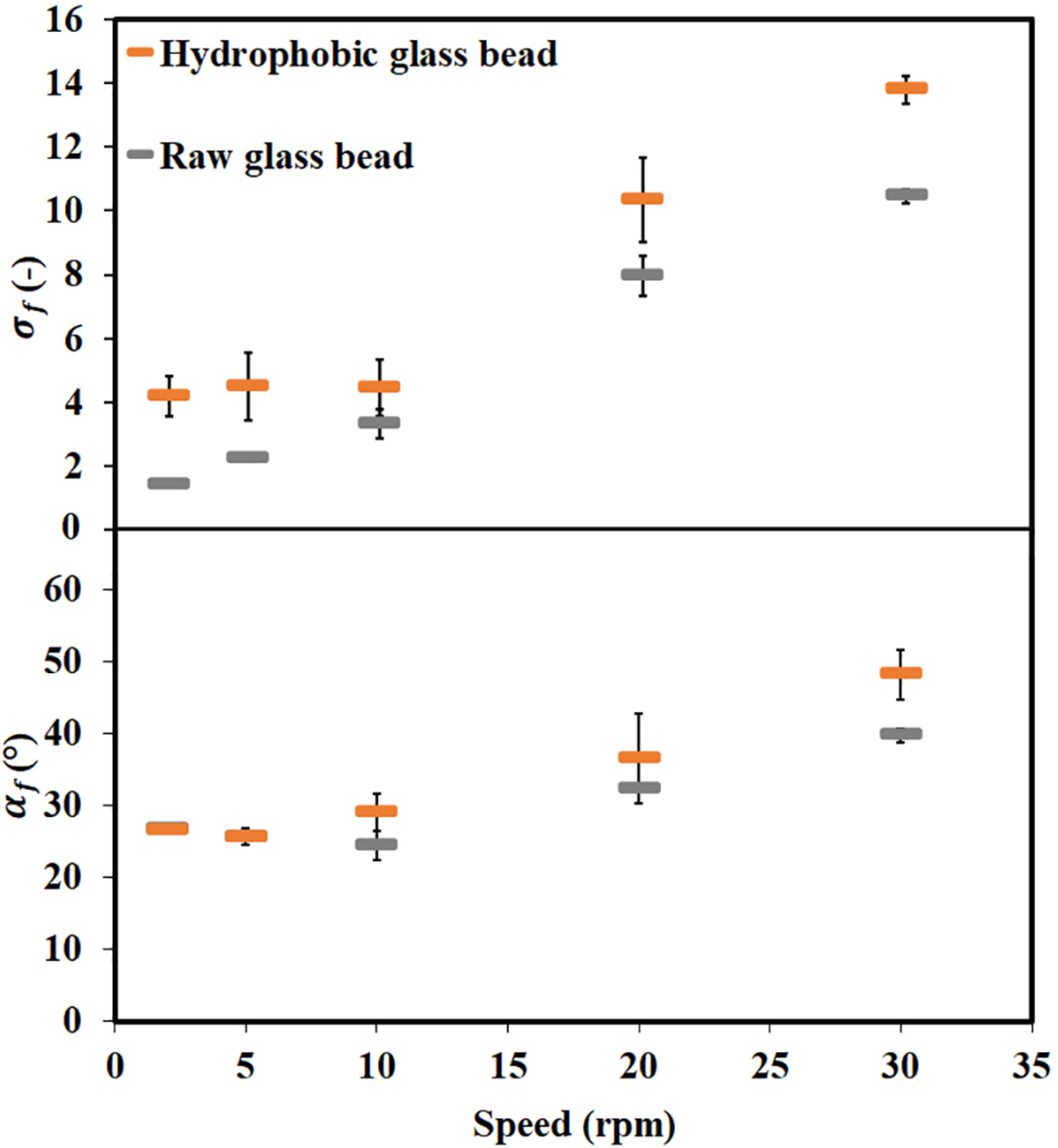
Hydrophobic glass bead
Raw glass bead
σ_f (-)
α_f (°)
Speed (rpm)
0
2
4
6
8
10
12
14
16
0
10
20
30
40
50
60
0
5
10
15
20
25
30
35

Figure 7

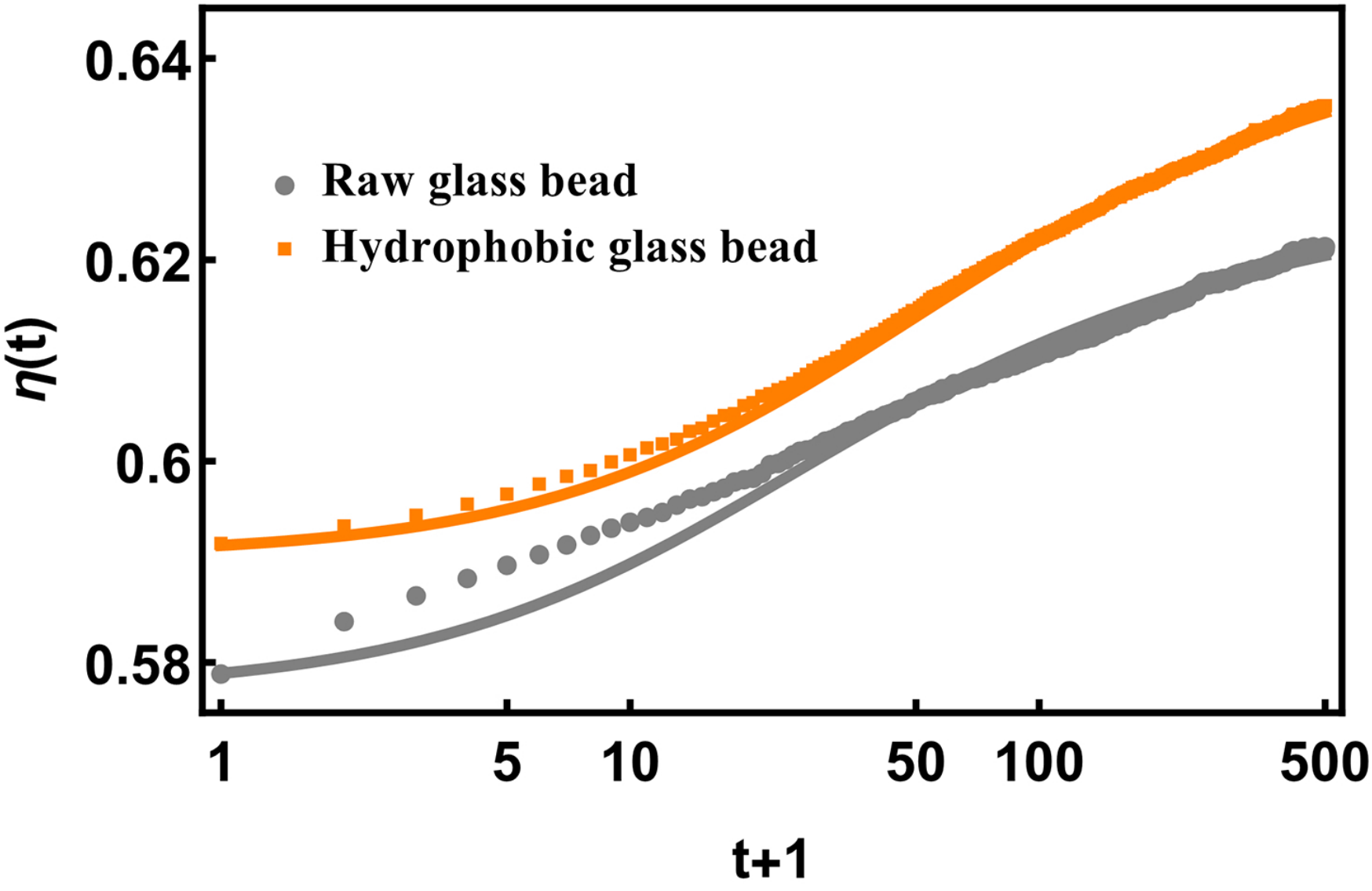
0.64
0.62
0.6
0.58
η(t)
Raw glass bead
Hydrophobic glass bead
1
5
10
50
100
500
t+1

Figure 8

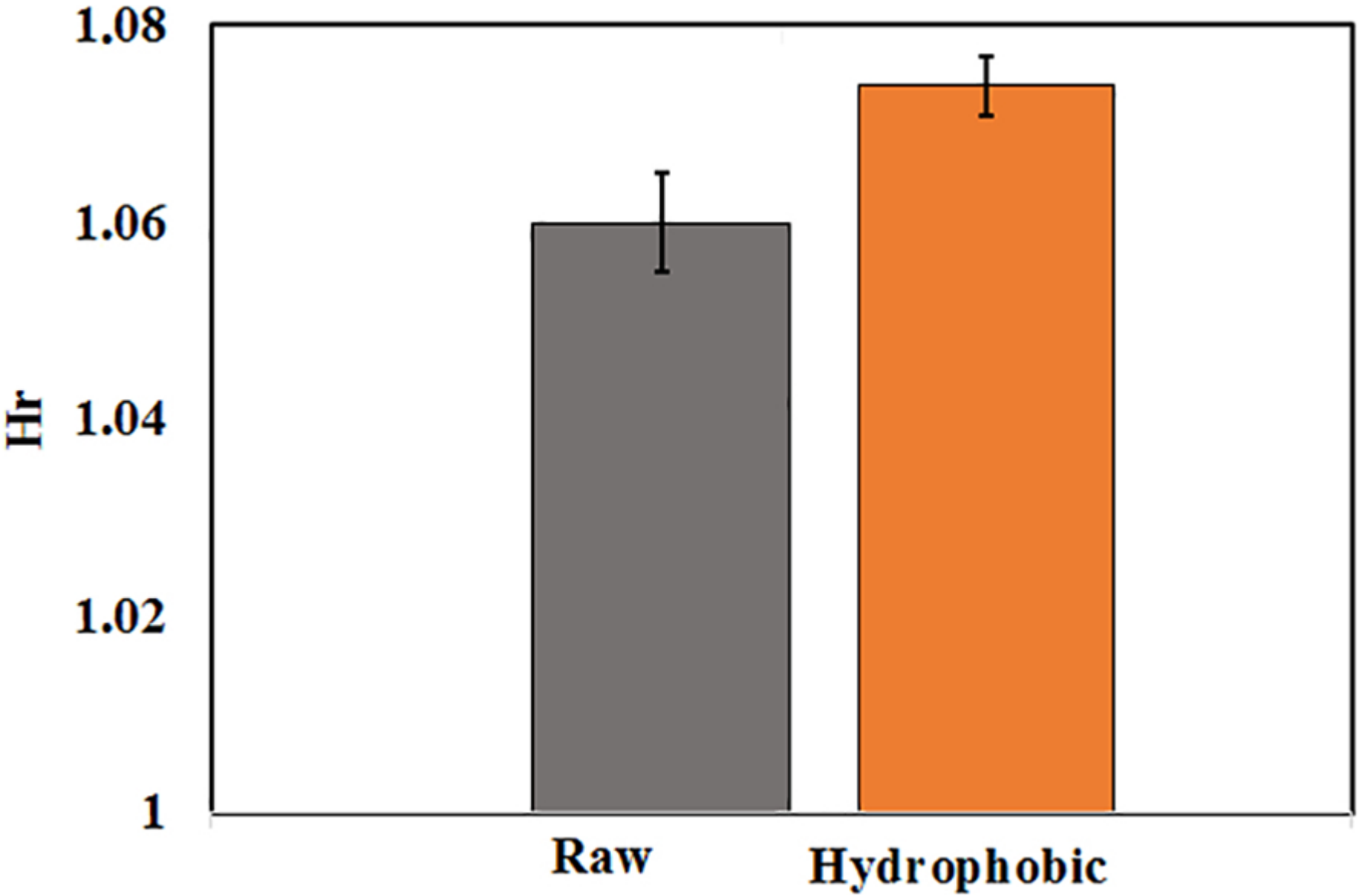

Figure 9

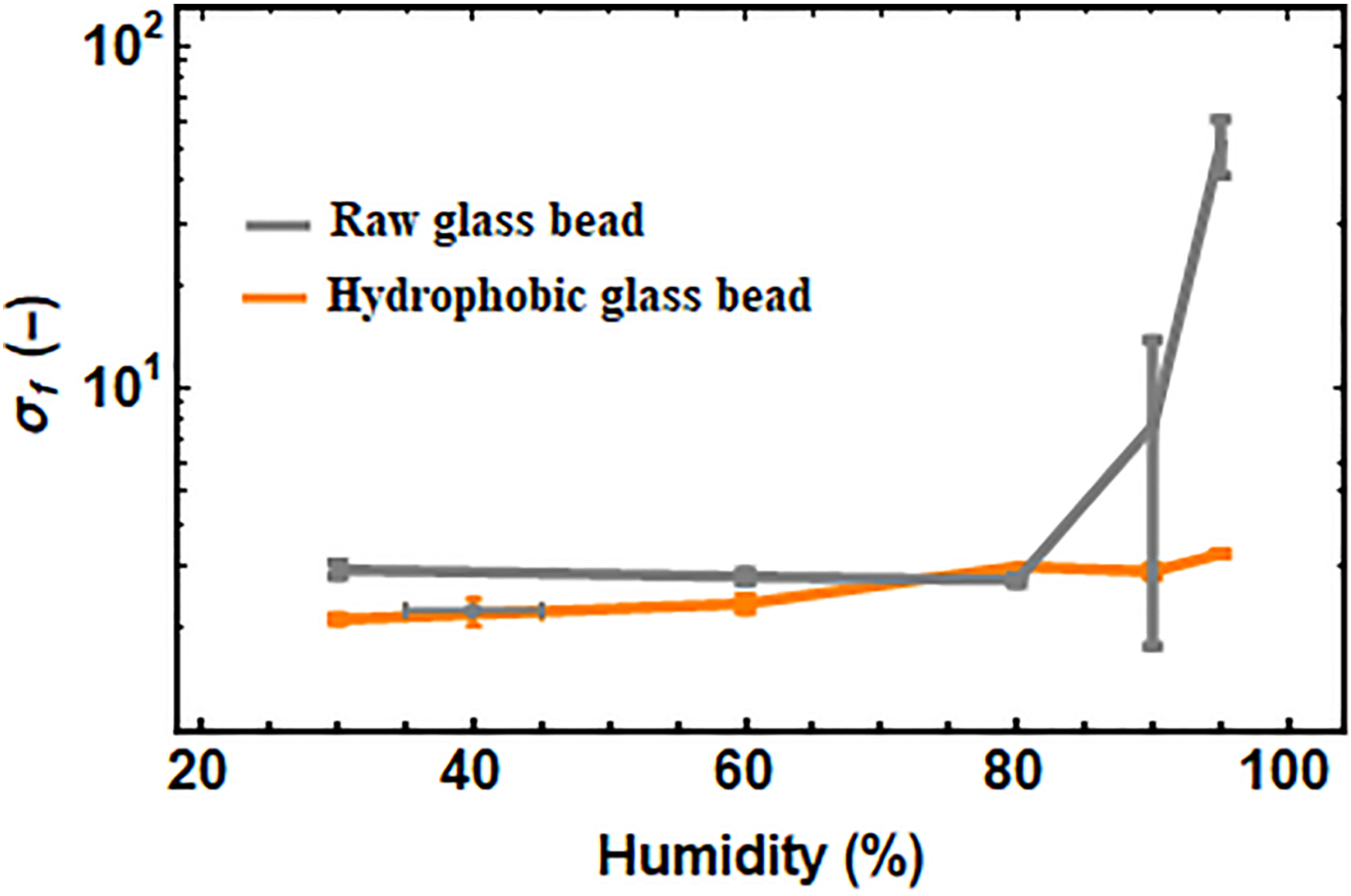
10^2
10^1
σ_f (-)
Raw glass bead
Hydrophobic glass bead
20
40
60
80
100
Humidity (%)

Figure 10

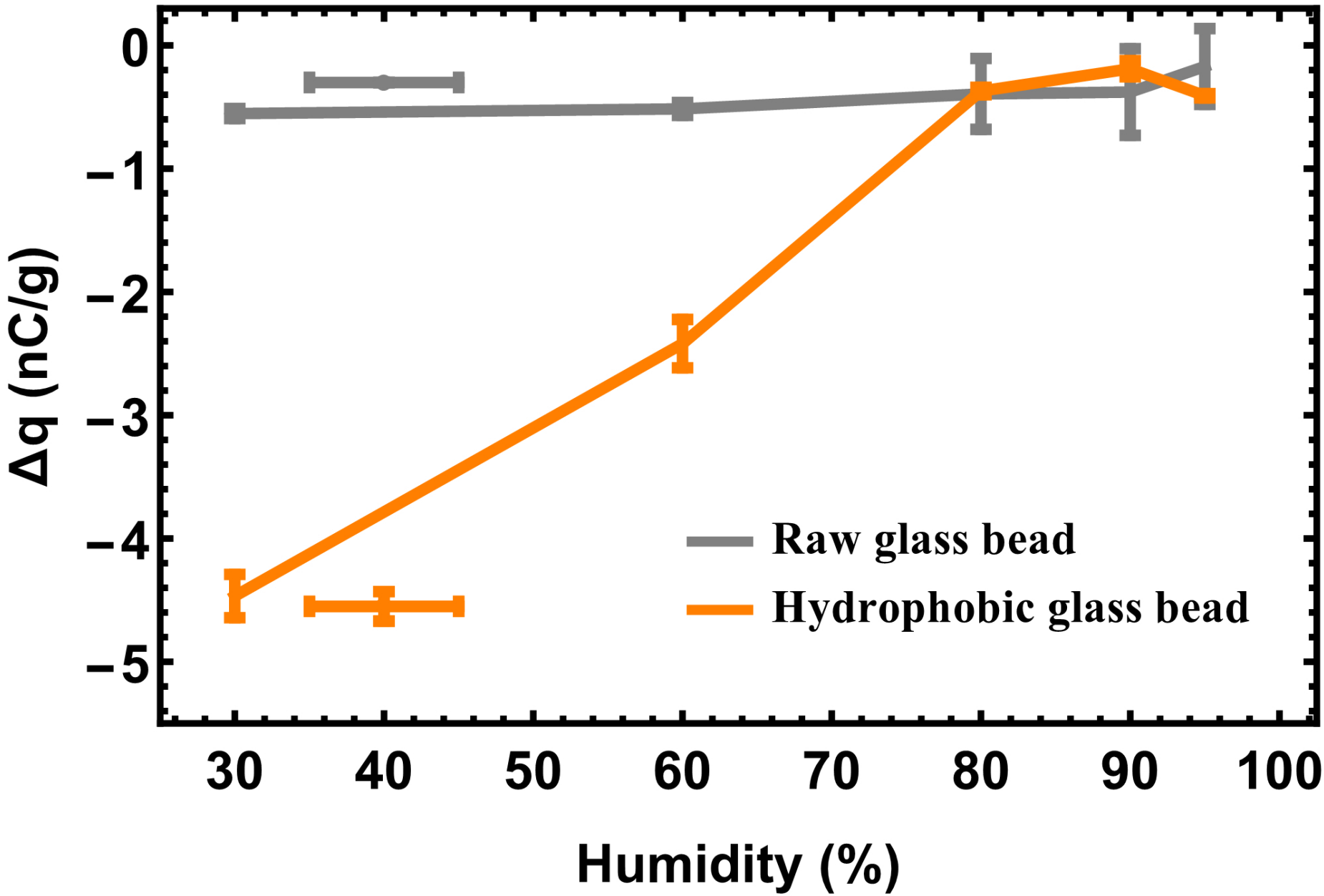
0
−1
−2
−3
−4
−5
Δq (nC/g)
30
40
50
60
70
80
90
100
Humidity (%)
Raw glass bead
Hydrophobic glass bead

Figure 11

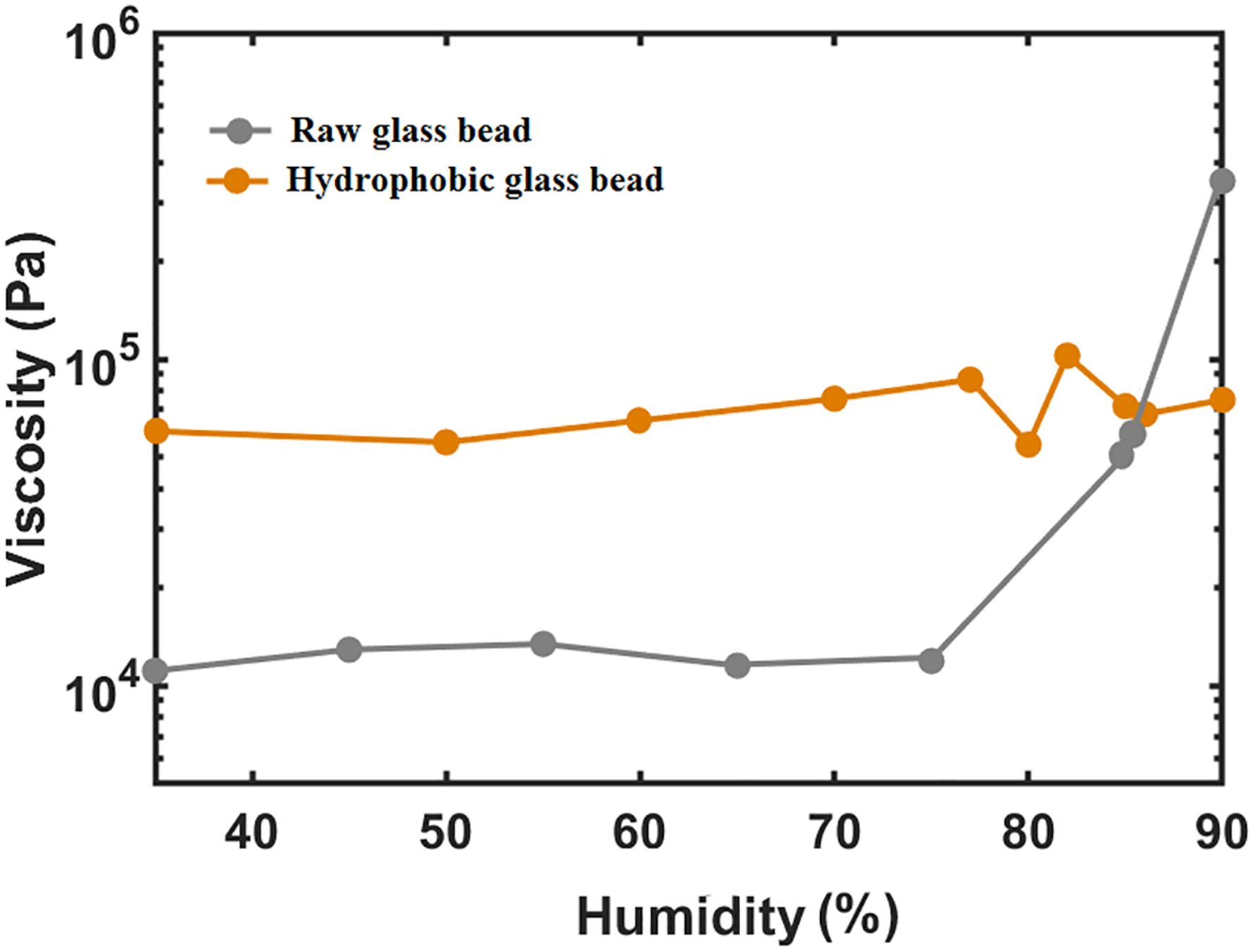
Raw glass bead
Hydrophobic glass bead
Viscosity (Pa)
10^6
10^5
10^4
40
50
60
70
80
90
Humidity (%)

Figure 12

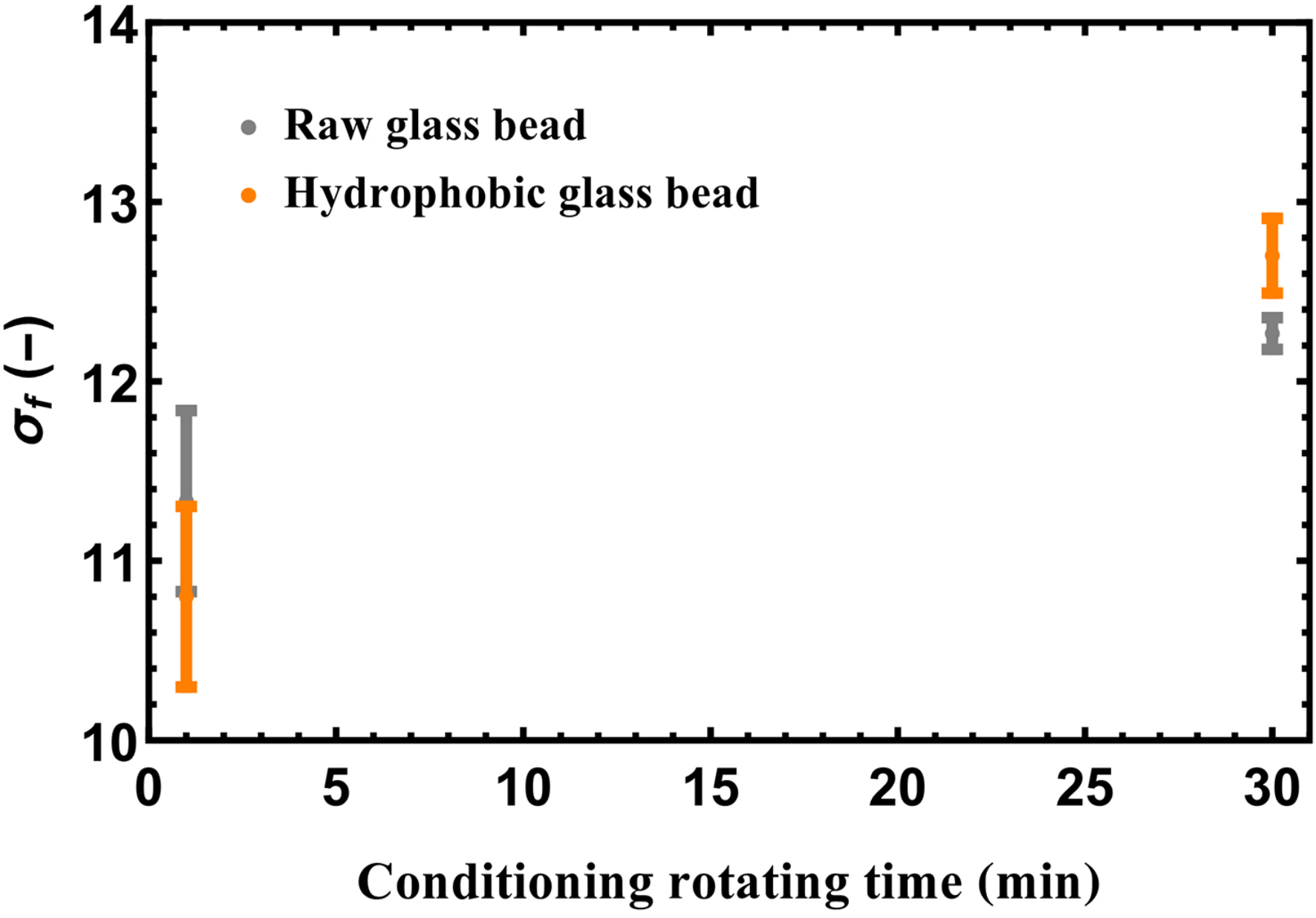
Raw glass bead
Hydrophobic glass bead
σ_f (-)
14
13
12
11
10
0
5
10
15
20
25
30
Conditioning rotating time (min)

Figure 13